

Pitting and Stress Corrosion Cracking Susceptibility of Nanostructured Al-Mg Alloys in Natural and Artificial Environments

Mala M. Sharma and Constance W. Ziemian

(Submitted June 13, 2007; in revised form December 29, 2007)

The stress corrosion cracking (SCC) behavior of two developmental nanocrystalline 5083 alloys with varied composition and processing conditions was studied. The results were compared to a commercial aluminum AA 5083 (H111) alloy. The pitting densities, size and depths, and residual tensile strengths were measured after alternate immersion in artificial seawater and atmospheric exposure under different loading conditions. Optical and scanning electron microscopy (SEM) with EDX was used to analyze the fracture surfaces of failed specimen after removal at selected intervals and tensile testing. One of the nanostructured Al-Mg alloys exhibited significantly superior pitting resistance when compared to conventional microstructured AA 5083. Under conditions where pitting corrosion showed up as local tunnels toward phase inclusions, transgranular cracking was observed, whereas under conditions when pitting corrosion evolved along grain boundaries, intergranular cracking inside the pit was observed. Pit initiation resistance of the nano alloys appears to be better than that of the conventional alloys. However, long-term pit propagation is a concern and warrants further study. The objective of this investigation was to obtain information regarding the role that ultra-fine microstructures play in their degradation in marine environments and to provide insight into the corrosion mechanisms and damage processes of these alloys.

Keywords aluminum, corrosion testing, failure analysis, mechanical testing

1. Introduction

Metals and alloys with grain sizes equal to or below 100 nm are defined as nanostructured (n-structured). Nanostructured materials (also described as nanocrystalline, nanophase, or nanoscale) have recently generated significant interest. This attention is due in part to the wide span of potential applications, from thermal barrier and wear resistant coatings to bulk structural materials. These materials exhibit dramatically altered properties because the grain size is also the same scale length as the phenomena, which gives rise to enhanced properties. Unfortunately, the limited data on nanomaterials is conflicting, especially with respect to corrosion performance. There is some evidence that nanoscale alloys can exhibit superior corrosion properties, especially in conditions where corrosion cracking, wear corrosion, and localized corrosion is important (Ref 1). Nanoscale alloys can be processed to yield a homogeneous microstructure, which makes the material less susceptible to failure by grain pull out or grain dropping (Ref 2, 3). The published facts regarding the corrosion resistance of bulk nanomaterials are virtually nonexistent. A number of nanoscale pure metal powders have been produced, but studies have found

them to be non-stable with regard to grain growth. A great deal remains to be learned about microstructural and grain growth control in these alloys. Nanomaterials are of significant interest to naval applications where high strength (and high strength-to-weight ratio), high temperature, and fatigue properties are required. Also of special interest for naval applications is the corrosion characteristics of these materials. Little research has been conducted to characterize the corrosion resistance of nanostructured materials, and the limited data that is available is somewhat conflicting (Ref 3-6). A careful study of the corrosion characteristics of nanostructured aluminum alloys is essential prior to their implementation in current and future designs.

In addition to the high strength, high temperature, and increased fatigue properties reported for these materials, corrosion properties are of particular interest for naval applications (Ref 7, 8). Nanomaterials may improve performance in applications where bulk materials are used in structures, components, and machinery and where service conditions subject the material to loading (static and cyclic) while in marine environments. However, this combined action of loading and aggressive environment often results in stress corrosion cracking (SCC) and ensuing damage that significantly reduces a material's fracture resistance. Since reduced fracture resistance can result in serious or catastrophic failure, a study of the SCC properties of this new class of materials is clearly necessary.

2. Experimental Procedure

Three alloys were used to study the effects of a finer grain size, composition and processing on the pitting and SCC mechanisms of aluminum alloys. The alloys used in this study

Mala M. Sharma and **C.W. Ziemian**, Department of Mechanical Engineering, Bucknell University, Dana Building, Lewisburg, PA 17837. Contact e-mail: msharjud@bucknell.edu.

are two developmental Al-Mg nanocrystalline alloys, Al-7.5Mg (extruded at a 20:1 ratio) and Al-8.6Mg (extruded at a 6.5:1 ratio), and a conventionally processed AA 5083-H111 Al-Mg alloy. The aluminum alloy AA5083-H111 can be classified as a wrought alloy product. Al 5083-H111 was chosen because of its common marine applications and excellent corrosion resistance. Currently, the Navy uses Al 5083 for all topside marine atmospheric exposure conditions. The temper was chosen based on similarity to the manufacturing process of the nanostructured alloy.

The Boeing Company in conjunction with the University of California, Irvine, synthesized the nanostructured alloys. They were produced through a combination of cryomilling and hot isostatic pressing. Spray atomized powders with particle sizes less than 150 μm were mechanically milled in liquid nitrogen to reduce the grain size. After cryomilling, the powder had a grain size of approximately 30 nm. The powder was then heated to 300 °C under a vacuum of 10^{-6} Torr for degassing. Consolidation was executed by hot isostatic pressing at 250 °C under a pressure of 200 MPa. The materials were then extruded at various extrusion ratios.

The compositions of the AA 5083-H111 and nanocrystalline Al-Mg alloys used in this study, in weight percent, are given in Table 1. Due to a limited supply of the developmental nanocrystalline alloys, not all materials were used for each method of testing. In order to help interpret the data obtained in this study, reference is made to previous work based on the localized corrosion behavior of these same nanocrystalline alloys (Ref 9).

2.1 Laboratory Long-term Constant Immersion

To investigate the role of grain size on pitting behavior, test coupons of the alloys were machined from extrusions in the longitudinal direction, according to the ASTM G-31 (Ref 10) standard. The final sample dimensions were $50.8 \times 25.4 \times 6.4$ mm ($2'' \times 1'' \times 0.25''$). Samples were placed in a beaker of artificial seawater (3.5% NaCl) and were fully immersed, partially immersed, and non-immersed (in vapor only, no contact with electrolyte). The beaker was closed to prevent evaporation and left alone for a period of 90 days. The samples were observed during the 90 day time period; the formation and location of pits was noted, weight loss and resulting corrosion rate was calculated after the end of the test. Samples were removed and cleaned as per the ASTM G-1 (Ref 11) standard, examined by optical and scanning electron microscopy (SEM).

2.2 Laboratory Long-term Alternate Immersion and Ocean Front Exposure

Smooth round specimens were machined in the LL orientation, where the loading axis paralleled the extrusion direction according to ASTM E-8 (Ref 12) standard. These specimens

Table 1 Composition of Al-Mg alloys investigated

	Alloy compositions, wt. %		
	5083 (H111)	Nano Al-7.5Mg	Nano Al-8.6Mg
Mg	4-4.9	7.5	8.6
Fe	<0.4	0.09	0.10
Cr	0.05-0.25	—	—
Mn	0.4-1	—	—

were used for tensile testing after laboratory alternate immersion. To evaluate the SCC susceptibility, samples were alternatively immersed for periods of 2 weeks, 1 month, 2 months, and 6 months in an unstressed condition according to ASTM G-44 (Ref 13) standard. In addition, specimens were loaded into stress frames at 50 and 75% of the respective material's yield strength and alternatively immersed for 6 months. The ASTM standard requires the immersion cycle to be 10 min of immersion and 50 min drying. The corrosive environment selected was a 3.5% NaCl solution. The temperature of the air in the cabinet was kept at 25 °C by a thermo regulator, and air was circulated by an electric heater and dehumidifier. A 12.7-mm (0.5") section of the specimen was exposed to the environment, and the rest was coated in epoxy to prevent the specimen from experiencing galvanic corrosion with the stress frame.

A separate set of specimens was exposed to ocean front atmosphere according to ASTM G-50 (Ref 14) standard. Specimens were placed on test racks exposed facing eastward (toward the Atlantic Ocean) positioned at a 30° angle from horizontal and were removed at time intervals of 2 months, 6 months, 1 year, and 2 years.

During the various exposure times, specimens were removed from the test environment and were examined weekly for signs of cracks or pitting using an optical microscope. Samples were removed at the allotted time intervals, cleaned, and a pitting analysis was conducted as per ASTM G-46 (Ref 15) guidelines.

Finally, the samples were tensile tested to obtain the residual strength measurements after alternate immersion. Tensile tests were conducted in laboratory air at a displacement rate of 2 mm/min by using a computer-controlled tensile testing Instron machine.

3. Results and Discussion

3.1 Laboratory Long-term Constant Immersion Testing

Figure 1 shows the SEM micrographs of the test coupons after 90 days of immersion in artificial seawater for the conventional AA 5083 and nano Al-7.5Mg alloys. For both the non-immersed and fully immersed conditions, very few pits were observed for both alloys tested. The greatest extent of degradation was observed in samples that were partially immersed, due to the constant source of oxygen at the electrolyte water line. A pitting analysis was conducted on these samples, where the size, number, and depth of the pits were noted, and the results are presented in Table 2.

For the most part, the number of pits and pit density between the nano alloys is comparable. The greatest variation between all the alloys occurred in the pit size, distribution and depth. The conventional alloy had pits which were irregularly shaped and clustered in various areas throughout the specimen. The average distribution of pits ranged in size from 0.5 to 1.7 mm^2 . Conversely, the nano alloys had slightly fewer, finer pits that were equiaxed in shape and ranged between 0.05-0.07 mm^2 and 0.04-0.06 mm^2 for the Al-7.5Mg and Al-8.6Mg alloys, respectively. In the nano alloys, the pits were more uniformly distributed throughout the samples, than observed for the conventional alloy, and had a narrower size distribution range. The conventional alloy appeared to have more significant damage do to pitting as far as quantity and size of pits.

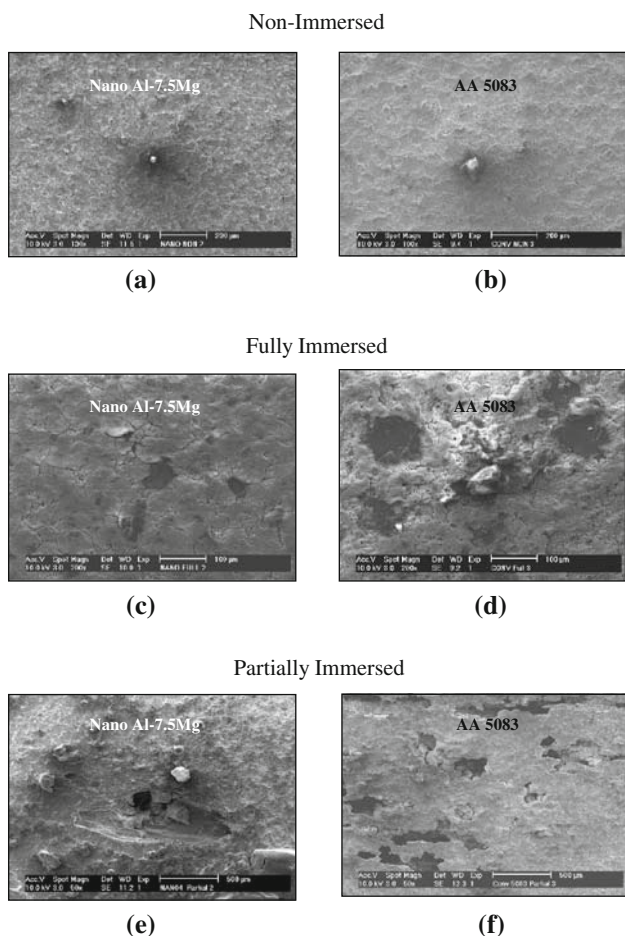


Fig. 1 SEM micrographs of the test coupons after 90 days immersion in artificial seawater for the nano Al-7.5Mg alloy (a, c, e) and the conventional 5083 alloy (b, d, f). Very few pits were observed in any of the three conditions and pictures are not exemplary of entire surface. The few pits that were observed are shown above

Table 2 Pitting analysis on partially immersed specimen

Alloy	# of Pits	Pit density (#/cm ²)	Pit size		Pit depth Avg, mm
			Max, mm ²	Min, mm ²	
Conv 5083	217	7.35	1.70	0.50	0.230
Nano Al-7.5Mg	207	7.00	0.07	0.05	0.410
Nano Al-8.6Mg	205	7.15	0.06	0.04	0.275

However, it was observed that the pit depth for the conventional material was only half that observed for the nano Al-7.5Mg alloy, and was closer in measurement to the nano Al-8.6Mg alloy. This behavior could possibly be explained by examining the data for the intergranular corrosion susceptibility of the nanocrystalline alloys. In a related study which examined the identical alloys (Ref 9), the intergranular corrosion susceptibility was investigated using the ASTM-67 (Ref 16) standard. According to the ASTM-67 (Ref 16) standard, alloys susceptible to intergranular corrosion should exhibit weight losses from 25 mg/cm², whereas alloys that are resistant to intergranular corrosion will only display weight losses between 1 and 5 mg/cm². The results revealed that the nanocrystalline alloys

were susceptible to intergranular corrosion, while the conventional AA 5083 was not. Specifically, it was observed that the grain boundaries of the nano Al-7.5Mg alloy was seriously corroded with many grains having fallen out while the grain boundaries of the conventional AA 5083 were left intact. Additionally, the corrosion attack was observed only around precipitates, not grain boundaries for the conventional alloy (Ref 9). This information helps to explain the variation in pitting depth observed between the conventional AA 5083 and nano Al-7.5Mg alloy. However, the rationale for less extensive pitting damage observed in the nano Al-8.6Mg alloy in regards to the pitting depth remains to be understood.

3.2 Tensile Fracture Behavior in Air and Artificial Seawater

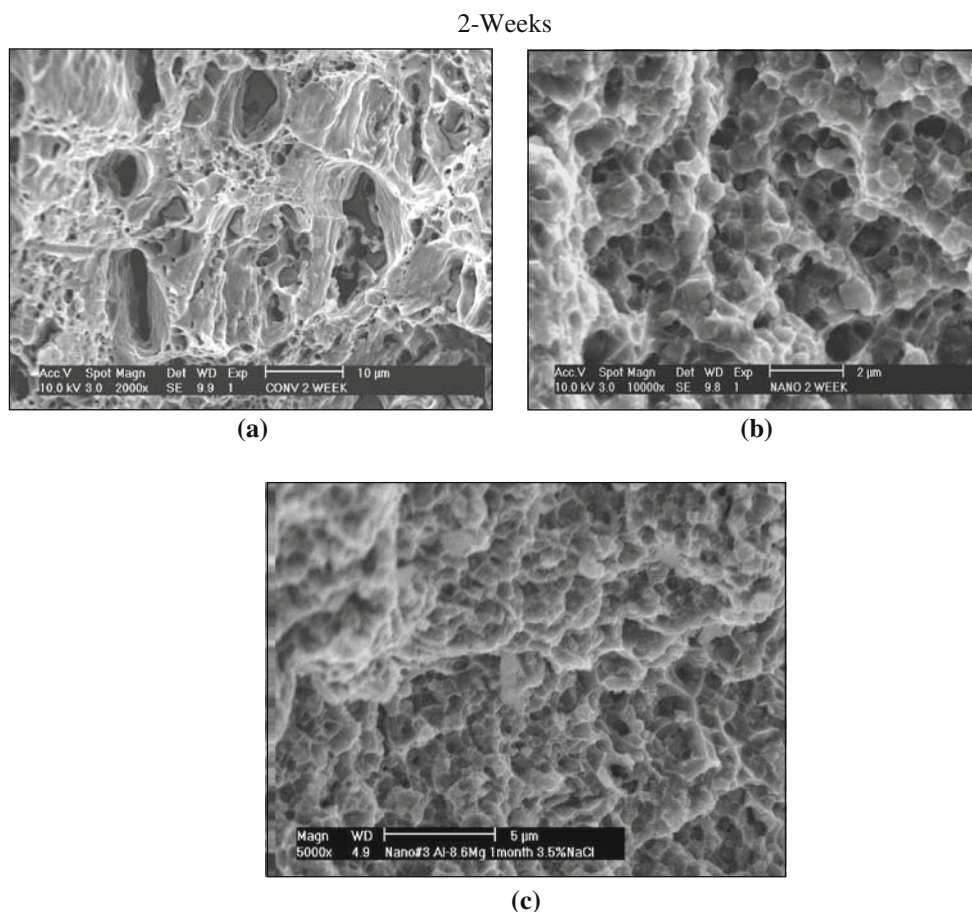
Table 3 summarizes the mechanical properties of specimen after laboratory alternate immersion testing. The yield strength, tensile strength, and percentage of residual strength retained after alternate immersion at various time intervals is presented. Percentage of residual strength retained was used as an indicator of stress corrosion attack, with lower percentages representing more significant susceptibility to corrosion attack. After alternate immersion of 2 weeks and 1 month, all three alloys retained the majority of their original strength. After 2 months, a noticeable decrease in strength was observed, and more significantly after 6 months, for the nano Al-7.5Mg and conventional AA5083 alloys, indicating the onset of corrosion attack. It is interesting to note that although the nano Al-7.5Mg alloy retained a higher percentage of residual strength over the conventional alloy, in both unstressed and 50% YS conditions, after 6 months of testing these same two alloys stressed to the 75% YS condition had comparable percentages of retained residual strength.

The nano Al-8.6Mg alloy maintained 91% of its residual strength during 1-6 months of testing, indicating little effect from corrosion cracking. Furthermore, when compared to the conventional AA5083, the alloy retained more than twice the percentage of residual strength after 6 months of alternate immersion in both the stressed and unstressed conditions. This is an interesting finding which indicates that the pitting kinetics of aluminum alloys may be dependant on grain size.

In order to understand the variation in stress corrosion behavior between all the alloys, an SEM examination of the fracture surfaces and a pitting analysis on the outside of the samples were conducted. Failure after samples were immersed from 2 weeks up to 1 month was purely by mechanical means and through ductile dimple rupture, Fig. 2(a)-(c). The SEM pictures also show failure by void coalescence and transgranular failure, no evidence of intergranular failure or failure initiating from pitting was observed. After 2 months of alternate immersion, the conventional alloy begins to show evidence of SCC through pitting. The main difference is displayed in the conventional alloy which appears to contain local tunnels directed toward phase inclusions, and transgranular cracking is observed near these areas. This can be seen in the micrographs presented in Fig. 3(a) and (b). Upon closer examination, there also appeared to be a difference in where and how the failure initiated between the alloys, see Fig. 4(a) and (b). For the conventional AA 5083, failure initiated at large inclusions where larger pits had formed around the inclusion. Examination of the failure surfaces clearly shows that the sizes of pits induced by the particles are almost always larger than the particle itself. This observation is consistent with cathodic

Table 3 Mechanical properties of alloys-alternate immersion

Alloy	Pre-exposure Unstressed	2 weeks Unstressed	1 month Unstressed	2 months Unstressed	6 months		
					Unstressed	50% YS	75% YS
<i>Yield strength, MPa (ksi)</i>							
5083-H111	269 (39)	255 (37)	221 (32)	145 (21)	124 (18)	110 (16)	97 (14)
Nano Al-7.5Mg	545 (79)	545 (79)	511 (74)	373 (54)	283 (41)	214 (31)	200 (29)
Nano Al-8.6Mg	524 (76)	N/A	504 (73)	497 (72)	449 (65)	386 (56)	359 (52)
<i>Tensile strength (ksi)</i>							
5083-H111	310 (45)	304 (44)	290 (42)	193 (28)	131 (19)	117 (17)	103 (15)
Nano Al-7.5Mg	580 (84)	559 (81)	517 (75)	379 (55)	310 (45)	283 (41)	200 (29)
Nano Al-8.6Mg	600 (87)	N/A	552 (80)	552 (80)	552 (80)	531 (77)	428 (62)
<i>% of Residual strength retained</i>							
5083-H111		97.8	93.3	62.2	42.2	37.7	33.3
Nano Al-7.5Mg		96.4	89.3	65.5	53.6	48.8	34.5
Nano Al-8.6Mg		N/A	91.1	91.1	91.1	88.5	71.2

**Fig. 2** SEM micrographs of fracture surfaces for conventional 5083 (a) nano Al-7.5Mg (b) and nano Al-8.6Mg (c)

behavior of constituent particles in the alloy, and may have been promoted by the Cr and Mn present in the alloy. In both the nano alloys, failure mostly initiated at uniform tiny pits which formed at very fine second phase particles, which are believed to be the strengthening β -phase Mg_2Al_3 . This composition was identified through SEM microprobe elemental analysis and EDX.

In commercial aluminum alloys, pitting corrosion has been observed to occur at intermetallic constituent particles. The role of constituent particles in the pitting corrosion of aluminum

alloys has been confirmed by many studies of 7075-T6 and 2024-T3 (bare) alloys in aerated 0.5 M NaCl solution (Ref 17, 18). There are two types of particles, type A and type C. Type A particles are anodic with respect to the matrix and tend to dissolve themselves, while type C particles are cathodic to the matrix and tend to promote dissolution of the adjacent matrix. In 7075-T6 and 2024-T3 alloys, the type A particles contain Al, Cu, and Mg, while those that contain Al, Cu, Fe, and Mn are type C particles. In this study from the SEM analysis, it appears that the conventional alloy contains more type C intermetallic

particles which dissolve the adjacent matrix and weaken the material when exposed to a corrosive medium. The nano alloys appear to contain finer type A particles which tend to dissolve themselves when exposed to a corrosive medium. The SEM

analysis identified these particles in samples before alternative immersion or atmospheric exposure. However, after exposure to corrosive mediums, SEM analysis revealed that second phase particles either dissolved themselves or dissolved the adjacent matrix. The variation in performance between the two nano alloys can be attributed to the location, size, distribution, and number of intermetallic and second phase particles (possibly related to the processing conditions of extrusion ratio and resulting grain size). Because these particles are important in promoting pitting corrosion, characterization of their crystal structure, chemical composition, and electrochemical behavior is needed to better understand the particle-pitting relationship.

In order to better understand the reasons for the variation in residual strength values between the alloys, a pitting analysis was conducted according to ASTM G-46 (Ref 15) standards for the alloys. Tables 4a-c show the pitting data for the alternate immersion SCC samples for the alloys. For all, the number of pits grew as exposure time increased. Average size and depth of pits also increased with time of exposure and stress level. The amount of increase varied with each respective alloy. For the nano Al-7.5Mg and conventional alloys, this increase was more dramatic with significant increases in pitting size and depth. However, the nano Al-8.6Mg alloy did not have as dramatic an increase in pitting size or depth. These findings were unexpected, but correlate well with residual strength results after alternate immersion. Despite the fact that the increased amount of magnesium in the nano Al-8.6Mg alloy promotes an increase of the intermetallic Mg_2Al_3 - β strengthening phase, thus allowing the alloy to remain stronger, it also provides additional sites for pitting, and larger, deeper pits would be expected. However, this alloy was also processed differently compared to the other alloys, and this processing history could have affected its performance.

Evidence for the reason behind the improved SCC resistance possessed by the nano 8.6Mg alloy over the nano Al-7.5Mg was again sought using scanning electron and optical microscopy. After 6 months in the unstressed condition, it was observed that the nano Al-7.5Mg alloy began to display evidence of corrosion cracking and exfoliation corrosion on the surface (Fig. 5), which are varieties of stress corrosion. Conversely, the nano 8.6Mg alloy displayed mostly small pits which had formed with little or no evidence of secondary cracking (Fig. 6). Figure 7 shows the nano Al-7.5Mg alloy in stressed in the 50% (a) and 75% (b) conditions showing evidence of significant transgranular secondary cracking near

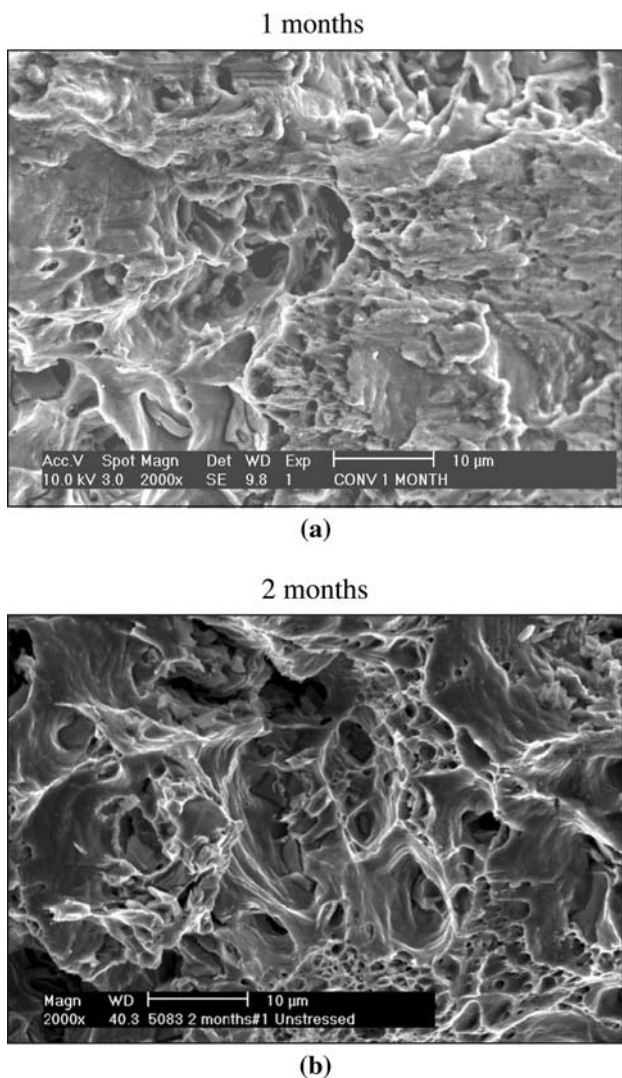


Fig. 3 (a, b) Conventional alloy showing signs of tunneling and transgranular failure due to the initiation of pitting corrosion

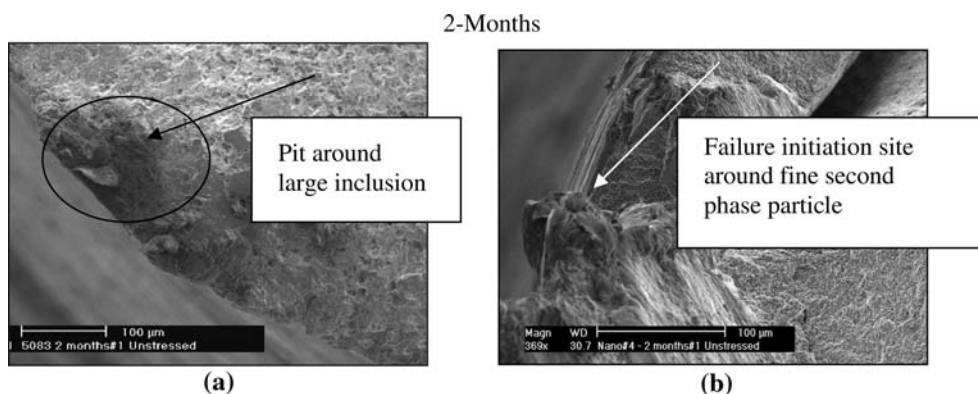


Fig. 4 SEM micrographs of fracture surfaces for (a) conventional AA 5083 and (b) nano Al-7.5Mg alloy after 2 months; close examination shows failure initiation point

Table 4 (a) Pitting analysis of conventional 5083 alternate immersion samples; (b) pitting analysis of nano Al-7.5Mg alternate immersion samples; and (c) pitting analysis of nano Al-8.6Mg alloy alternate immersion samples

	Pit density Avg, #/cm ²	Pit surface area Avg, mm ²	Pit depth	
			Avg, mm	Max, mm
(a)				
Alloy				
<i>Unstressed</i>				
2 months	14	<0.004	0.0035	0.004
6 months	17	<0.008	0.0066	0.008
<i>Stressed</i>				
50%	24	<0.02	0.0108	0.013
75%	13	<0.03	0.0117	0.015
(b)				
Time				
<i>Unstressed</i>				
2 months	5.7	<0.0008	0.0045	0.005
6 months	13.7	<0.0070	0.0182	0.029
<i>Stressed</i>				
50%	26	<0.009	0.0264	0.031
75%	8.7	<0.02	0.0458	0.052
(c)				
Alloy				
<i>Unstressed</i>				
2 months	6	<0.0004	0.0036	0.004
6 months	14	<0.002	0.0044	0.006
<i>Stressed</i>				
50%	17	<0.004	0.0085	0.009
75%	10	<0.007	0.0116	0.012

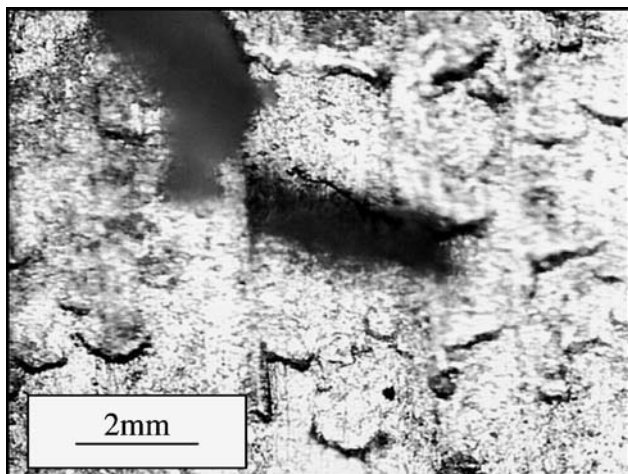


Fig. 5 Optical micrograph of nano Al-7.5Mg Alloy after 6 months of testing in 3.5% NaCl solution in the unstressed condition. Evidence of intergranular and exfoliation corrosion cracking on the outer surface of the specimen is obvious

pits, which is the attributing factor that led to the decrease in residual strength in this particular nano alloy. The extent of corrosion is consistent with the previous observations which suggested particle dissolution and pit propagation of corrosion. No significant evidence of corrosion cracking on the surface of the nano Al-8.6Mg alloy was noted. However, inside a pit

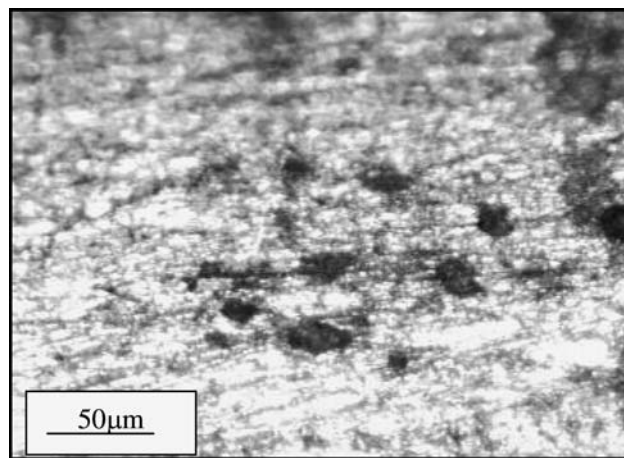
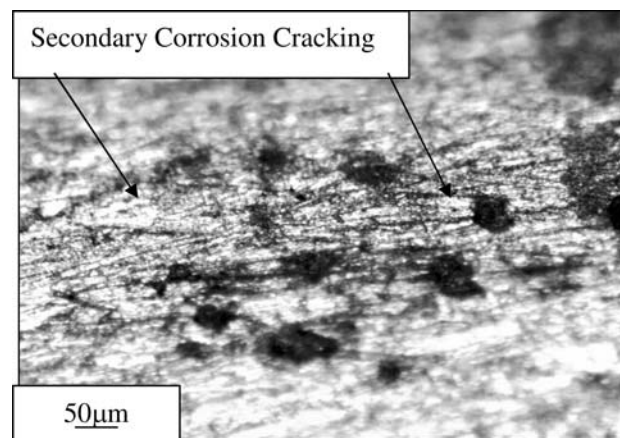
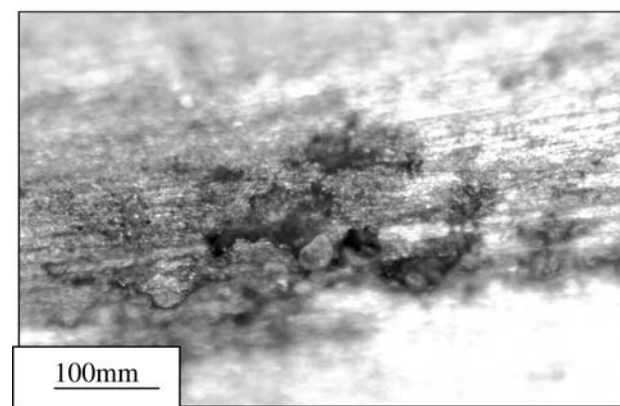


Fig. 6 Optical micrograph of nano Al-8.6Mg showing very little evidence of secondary cracking on the surface of the sample after 6 months of testing in 3.5% NaCl solution. Pits are fine and evenly distributed



(a)



(b)

Fig. 7 Optical micrograph of nano Al-7.5Mg showing evidence of enhanced pitting and resulting secondary corrosion cracking which led to a significant decrease in residual strength in this alloy after alternate immersion for 6 months stressed to (a) 50% and (b) 75% of the material's yield strength. Cracks are essentially transgranular

where failure initiated, evidence of intergranular corrosion is obvious (Fig. 8). Under conditions where pitting corrosion evolves on grain boundaries, only intergranular cracking is observed (Ref 19). Again, the principal mechanism for the growth of more severe corrosion pits is believed to be attributed to the distribution and location of second phase particles and inclusions.

The SEM micrographs help to explain the enhanced stress corrosion resistance displayed by the nano Al-8.6Mg alloy over the other two alloys. If this improved behavior is related to refined grain size, composition, an effect from processing, or a combination thereof, however, is yet to be established. Grain sizes from the related study (Ref 9) established that many of the grains in the Al-7.5Mg and Al-8.6Mg alloy were in fact not nanocrystalline by definition. Some grains were found to be nano sized where others were larger. The grain sizes for both alloys ranged between 300 and 500 nm. However, many grains ranging from 30 to 80 nm were also observed for the alloys (Ref 20).

The results of the pitting analysis for the ocean front exposure samples are presented in Tables 5 and 6. Similar to

the previous results, the conventional material had a much higher pitting density than the nano Al-7.5Mg alloy for both the 6 month and 1 year atmospheric exposures; samples exposed for up to 2 years were too difficult to analyze due to build up of corrosion product on the samples and accurate pitting data was not obtained. The greatest variation in data was again in the maximum and average pit depth. Even though the nano Al-7.5Mg alloy had fewer pits, the depth was 3-4 times greater compared to the conventional alloy after 6 months of atmospheric ocean front testing. These results differ significantly from those reported for Kus et al. (Ref 21) who found their conventional 5083 to have fewer, but larger pits after exposure. This behavior may be explained using the results of the intergranular corrosion susceptibility test, ASTM-67 (Ref 9, 16). After 1 year of atmospheric testing, this trend was not as obvious, maximum and average pit depths were comparable between the two alloys. This behavior suggests that the pitting kinetics of the nano and conventional alloys are quite different. The results also show that the nano alloys have a greater susceptibility to intergranular corrosion, and thus intergranular fall out, again contrary to that reported for Kus et al. (Ref 21). Although a higher susceptibility to intergranular corrosion is not necessarily required for greater pit depths or higher pitting kinetics, from the SEM observations, it is believed that intergranular corrosion can accompany intergranular pitting (Ref 19) and promote deeper pits. The deeper pits experienced by the nano Al-7.5Mg alloys after short-term, alternate immersion and atmospheric exposure when compared to the conventional alloy can be explained through the SEM observations. The transgranular secondary corrosion cracking observed in the nano Al-7.5Mg alloys led to the deeper pits and reduced residual strength. However, if this is true then based on the intergranular results from a previous study (Ref 9), the nano Al-8.6 Mg should have a greater degree of corrosion attack. But, as previously stated, this was not the case and is believed to be attributed to the location and distribution of second phase particles and lack of inclusions in the nano Al-8.6Mg alloy. Hence, in spite of the fact that pitting corrosion and corrosion cracking essentially differ in mechanism, they similarly correlate with the structure of alloys and their fracture and failure patterns. Overall it can be concluded that the transgranular cracking of the nano alloys can take place when pitting occurs in the form of narrow channels, whereas the

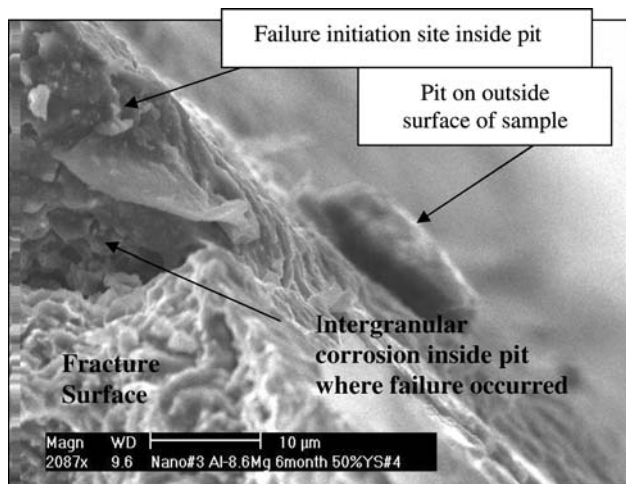


Fig. 8 SEM micrographs of nano Al-8.6Mg alloy after 6 months of alternate immersion in 3.5% NaCl in the 50% YS condition. Inside the pit intergranular corrosion is obvious

Table 5 Pitting analysis of 6-month atmospheric exposure unstressed samples

Alloy	Pit density Avg, #/cm ²	Pit surface area Avg, mm ²	Pit depth		Depth 6 deepest Avg, mm	ASTM G46 rating
			Avg, mm	Max, mm		
5083	>50	<0.5	<0.4	<0.01	<0.010	>A5, <B1, <C1
Nano Al-7.5Mg	10 > 50	<0.5	<0.4	0.04	<0.029	A4, <B1, <C1

Table 6 Pitting analysis of 1 year atmospheric exposure unstressed samples

Alloy	Pit density Avg, #/cm ²	Pit surface area Avg, mm ²	Pit depth		Depth 6 deepest Avg, mm	ASTM G46 rating
			Avg, mm	Max, mm		
5083	>50	<0.5	<0.4	0.053	0.027	>A5, <B1, <C1
Nano Al-7.5Mg	10 > 50	<0.5	<0.4	0.057	0.041	A4, <B1, <C1

intergranular corrosion cracking accompanies a grain-boundary pitting mechanism.

From this data, it can be hypothesized that over time, in general, pit propagation slows down for the nano alloys while it increases for the conventional alloy. This suggests that not only are the pitting kinetics of the nano and conventional alloys quite different, but the pitting kinetics may also be affected by various processing parameters, chemical composition, and grain size. To confirm this hypothesis and to completely understand this phenomenon, an investigation into the pitting kinetics of these alloys is necessary. Electrochemical testing was conducted in a related and previously executed study by Sikora et al. (Ref 9). The results can be used to elucidate this varied behavior.

When evaluating the susceptibility of a material to pitting corrosion, two important factors should be considered: the nucleation of new pits and growth or repassivation of pre-existing pits. In the study by Sikora et al. (Ref 9), it was found that the value of E_p , the pitting potential, was significantly affected by extrusion ratio, whereas E_{oc} (open circuit potential) and i_p (passive current density) were not as linked to processing condition. The protection potentials [defined as the potential at which the current is zero on the reverse scans (Ref 22) or as the potential below which no pitting occurs and above which pit that have already nucleated can grow (Ref 23)] measured for the nano alloys were also found to be unaffected by differing compositions or extrusion ratios. Since the nanocrystalline alloys studied herein differ not only in grain size, but also chemical composition, it is difficult to establish the specific factors that influence the electrochemical behavior of the various nanocrystalline alloys. However, the results from Sikora et al. (Ref 9), and the current study, prompt the conclusion that during the repassivation process, the grain size and amount of grain boundary do play a significant role (Ref 24, 25).

Sikora et al. (Ref 9) also used cyclic polarization experiments to evaluate the pitting behavior of the nano Al-7.5Mg and nano Al-8.6Mg alloys. It was observed that the nano Al-8.6Mg alloy had a slightly higher degree of protection compared to the nano Al-7.5Mg alloy, against pit nucleation in chloride environments and this protection increased with increasing chloride concentration. These results correlate well with the SEM observations and pitting analysis of the corroded surfaces in the present study which showed the nano Al-7.5Mg alloy to have an improved resistance to stress corrosion versus the conventional AA 5083, but more significant pitting damage compared to the nano Al-8.6Mg alloy. The resistance against the growth of preexisting pits (or the ability to repassivate) was also evaluated by Sikora et al. (Ref 9) by comparing areas of the anodic hysteresis loops obtained from cyclic polarization diagrams (the area is related to electrochemical charge consumed during the growth of the pre-existing pits). It was observed that in a deaerated solution of 0.1 M Na_2SO_4 + 0.5 M NaCl, the electrochemical charge consumed during growth of pits was much lower in the nano Al-8.6Mg alloy than for the nano Al-7.5Mg alloy. Again, these results correlate with the pitting analysis of the current study, which found variations in the distribution, size, and depth of pits for both of these alloys. These findings would indicate that not only does grain boundary area have a significant effect on stress corrosion behavior; but the size, composition, and distribution of second phase and intermetallic particles have a direct effect on the pitting and thus SCC resistance of Al-Mg-based alloys.

4. Conclusions

The nano Al-8.6Mg alloy exhibited significantly superior pitting resistance in the short term when compared to microstructured conventional AA 5083. Both nano Al-7.5Mg and nano Al-8.6Mg alloys had fewer and finer pits compared to the conventional alloy. During times of exposure between 1 and 6 months, deeper pits in the nano Al-7.5Mg nanocrystalline alloy was predominantly attributed to intergranular fall out and intergranular pitting. However, with increased testing periods, pitting depths for all alloys were comparable and are attributed to the increased ability of the nano alloys to repassivate. While the pit initiation resistance of the nano alloys appears to be better than that of the conventional alloys, pit propagation data varied between the two nano alloys, and this phenomena is a concern and warrants further study.

The SCC performance of the nano Al-7.5Mg alloy compares well with the AA 5083 alloy. The performance of the nano Al-8.6Mg is even better and this alloy appears to be more resistant to stress corrosion. This improved stress corrosion resistance is believed to be due to the composition and processing variation, in addition to finer grain size. Further investigation must be conducted comparing the corrosion behavior of nanocrystalline and conventional alloys of the same composition and processing techniques.

Acknowledgments

This work was sponsored by the Office of Naval Research (ONR) grant # N00014-00-1-0153 and NACE international seed grant # N000140210024. The authors would also like to thank The LaQue Testing and Research Center for their assistance in testing and analysis, and Boeing Corporation and E. Lavernia at University of California-Irvine for providing the nanostructured alloys. Many thanks are also extended to Barbara Shaw and Ela Sikora who collaborated on this ONR project.

References

1. V. Tellkamp and E. Lavernia, Processing and Mechanical Properties of Nanocrystalline 5083 Al Alloy, *Nanostruct. Mater.*, 1999, **12**, p 249–254
2. U. Erb, G. Palumbo, R. Zugic, and K.T. Aust, *Processing and Properties of Nanocrystalline Materials*, C. Suryanarayana, Ed., TMS, **93**, 1996
3. C. Cheung, D. Wood, and U. Erb, *Processing and Properties of Nanocrystalline Materials*, C. Suryanarayana, Ed., TMS, 1996, p 479–491
4. R.B. Inturi and Z. Szklarska-Smialowska, Localized Corrosion of Nanocrystalline 304 Type Stainless Steel Films, *Corrosion*, 1992, **48**, p 398–405
5. O. Elkedim, H.S. Cao, and P. Fluzin, Hardness and Corrosion Performance of Nanocrystalline Iron Powder Prepared by Ball Milling, *Mater. Sci. Forum*, 1999, **312–314**, p 635–640
6. W. Zieger, M. Schneider, and H. Worch, Passivity and Pitting Corrosion of a Nanocrystalline FeAl-8 Alloy, *Mater. Sci. Forum*, 1998, **269–272**, p 833–836
7. J.C. Chang and T.H. Chuang, Stress-Corrosion Cracking Susceptibility of the Superplastically Formed 5083 Aluminum Alloy in 3.5 pct NaCl Solution, *Metall. Mater. Trans. A*, 1999, **30A**, p 3191–3199
8. R. Verma, A.K. Ghosh, S. Kim, and C. Kim, Grain Refinement and Superplasticity in 5083 Al, *Mater. Sci. Eng.*, 1995, **191A**, p 143–156
9. E. Sikora, X.J. Wei, and B.A. Shaw, Corrosion Behavior of Nanocrystalline Bulk Al-Mg-Based Alloys, *Corrosion*, 2004, **60**(4), p 387–397
10. ASTM G31-72, Standard Practice for Laboratory Immersion Corrosion Testing of Metals, *Book of Standards Vol. 3.02*, ASTM International, West Conshohocken, PA, 2004, www.astm.org

11. ASTM G1-03, Standard Practice for Preparing, Cleaning, and Evaluating Corrosion Test Specimens, *Book of Standards Vol. 3.02*, ASTM International, West Conshohocken, PA, www.astm.org
12. ASTM E8-04, Standard Test Methods for Tension Testing of Metallic Materials, *Book of Standards Vol. 3.01*, ASTM International, West Conshohocken, PA, www.astm.org
13. ASTM G44-99, Standard Practice for Exposure of Metals and Alloys by Alternate Immersion in Neutral 3.5% Sodium Chloride Solution, *Book of Standards Vol. 3.02*, ASTM International, West Conshohocken, PA, 2005, www.astm.org
14. ASTM G50-76, Standard Practice for Conducting Atmospheric Corrosion Tests on Metals, *Book of Standards Vol. 3.02*, ASTM International, West Conshohocken, PA, 2003, www.astm.org
15. ASTM G46-94, Standard Guide for Examination and Evaluation of Pitting Corrosion, *Book of Standards Vol. 3.02*, ASTM International, West Conshohocken, PA, 2005, www.astm.org
16. ASTM G67-04, Standard Test Method for Determining the Susceptibility to Intergranular Corrosion of 5XXX Series Aluminum Alloys by Mass Loss After Exposure to Nitric Acid (NAMLT Test), *Book of Standards Vol. 3.02*, ASTM International, West Conshohocken, PA, www.astm.org
17. G.S. Chen, D.J. Harlow, and R.P. Wei, FAA/NASA, *Inst. Symp. on Advanced Structure Integrity Methods for Airframe Durability and Damage Tolerance*, NASA Conference Publication 3274, Langley Research Center, Hampton VA, Sept. 1994, p 157
18. G.S. Chen, M. Gao, and R.P. Wei, Micro-Constituents Induced Pitting Corrosion in a 2024-T3 Aluminum Alloy, *Corrosion*, 1996, **52**, p 8
19. V.S. Sinyavskii, Pitting and Stress Corrosions of Aluminum Alloys; Correlation Between Them, *Prot. Met.*, 2001, **37**(5), p 521–530
20. V.L. Tellkamp, A. Melmed, and E.J. Lavernia, Mechanical Behavior and Microstructure of Thermally Stable Bulk Nanostructured Al Alloy, *Metall. Mater. Trans. A*, 2001, **32A**, p 2335–2343
21. E. Kus, Z. Lee, S. Nutt, and F. Mansfeld, A Comparison of the Corrosion Behavior of Nanocrystalline and Conventional Al 5083 Sample, *Corrosion*, 2006, **62**(2), p 152–161
22. C. Vanleughenaghe, L. Klimzack-Mathieu, J. Meunier, and M. Porbaix, *Corros. Sci.*, 1962, **2**, p 69
23. M. Bethencourt, F.J. Botana, M.A. Cauqui, M. Marcos, M.A. Rodriguez, and J.M. Rodriguez-Izquierdo, Protection Against Corrosion in Marine Environments of AA5083 Al-Mg Alloy by Lanthanide Chlorides, *J. Alloy Compd.*, 1997, **250**, p 98
24. D. Witkin, B.Q. Han, and E.J. Lavernia, Room-Temperature Mechanical Behavior of Cryomilled Al Alloys, *Metall. Mater. Trans. A*, 2006, **37A**, p 185–194
25. S.Y. Chang, B.D. Ahn, S.K. Hong, S. Kamado, Y. Kojima, and D.H. Shin, Tensile Deformation Characteristics of a Nano-structured 5083 Al Alloy, *J. Alloy Compd.*, 2005, **386**, p 197–201